

Anisotropic Magnetoresistivity in Semimetal TaSb<sub>2</sub> \*

Xia-Yin Liu(刘夏吟)<sup>1</sup>, Jia-Lu Wang(王嘉璐)<sup>2</sup>, Wei You(尤伟)<sup>2</sup>, Ting-Ting Wang(王婷婷)<sup>2</sup>,  
 Hai-Yang Yang(杨海洋)<sup>2</sup>, Wen-He Jiao(焦文鹤)<sup>1</sup>, Hong-Ying Mao(毛宏颖)<sup>2</sup>, Li Zhang(张莉)<sup>3</sup>,  
 Jie Cheng(程杰)<sup>4</sup>, Yu-Ke Li(李玉科)<sup>2\*\*</sup>

<sup>1</sup>Department of Physics, Zhejiang University of Science and Technology, Hangzhou 310023

<sup>2</sup>Department of Physics and Hangzhou Key Laboratory of Quantum Matters, Hangzhou Normal University, Hangzhou 310036

<sup>3</sup>Department of Physics, China Jiliang University, Hangzhou 310018

<sup>4</sup>College of Science, Center of Advanced Functional Ceramics, Nanjing University of Posts and Telecommunications, Nanjing 210023

(Received 22 September 2017)

We investigate the anisotropic magnetic transports in topological semimetal TaSb<sub>2</sub>. The compound shows the large magnetoresistance (MR) without saturation and the metal-insulator-like transition no matter whether the magnetic field is parallel to *c*-axis or *a*-axis, except that the MR for  $\mathbf{B} \parallel c$  is almost twice as large as that of  $\mathbf{B} \parallel a$  at low temperatures. The adopted Kohler's rule can be obeyed by the MR at distinct temperatures for  $\mathbf{B} \parallel c$ , but it is slightly violated as  $\mathbf{B} \parallel a$ . The angle-dependent MR measurements exhibit the two-fold rotational symmetry below 70 K, consistent with the monoclinic crystal structure of TaSb<sub>2</sub>. The dumbbell-like picture of angle-dependent MR in TaSb<sub>2</sub> suggests a strongly anisotropic Fermi surface at low temperatures. However, it finally loses the two-fold symmetry over 70 K, implying a possible topological phase transition at around the temperature where  $T_m$  is related to a metal-insulator-like transition under magnetic fields.

PACS: 75.30.Gw, 73.43.-f, 71.30.+h, 75.47.De

DOI: 10.1088/0256-307X/34/12/127501

The study of magnetoresistance (MR) has become one of the most important topics in condensed matter physics. The MR not only gives information about the characteristics of the Fermi surface<sup>[1]</sup> but also is of vital importance to practical applications such as magnetic sensors, magnetic memory and hard drives.<sup>[2,3]</sup> Generally, a large MR is expected to be discovered in the magnetic materials like multilayer films<sup>[4]</sup> and Mn-based perovskites,<sup>[5]</sup> where the large MR originates from the magnetic mechanism. Interestingly, a number of non-magnetic metals have been recently discovered to exhibit the extremely large MR (XMR), such as Cd<sub>3</sub>As<sub>2</sub>,<sup>[6]</sup> WTe<sub>2</sub>,<sup>[7]</sup> TaAs-family<sup>[8–17]</sup> and ZrSiS.<sup>[18,19]</sup> In comparison with the conventional metals with a small MR of about a few percentages, those materials possess the XMR without saturation at rather high magnetic fields. Several possible mechanisms have been proposed to explain its origin: (1) the linear energy dispersion of Dirac fermions leading to the quantum limit;<sup>[20]</sup> (2) the compensated electron-hole carrier density;<sup>[7,10]</sup> and (3) the topological protection mechanism.<sup>[21]</sup>

Very recently, a new family of topological semimetals (TSMs), the transition-metal dipnictides  $XPn_2$  ( $X = \text{Ta, Nb, Mo, Pn} = \text{P, As, Sb}$ ), which crystallize in a centro-symmetry monoclinic structure, have been discovered and investigated.<sup>[22–24]</sup> The  $XPn_2$ -type compounds share some exotic transports such as the XMR and the ultrahigh electronic mobility.<sup>[25–28]</sup> In particular, the robust low-temperature resistivity

plateau and negative MR against the applied magnetic fields,<sup>[22,25,29]</sup> which are likely attributed to the disentangled bulk electron/hole bands and topological non-trivial surface states,<sup>[30]</sup> are observed. Following those results, the new members MoAs<sub>2</sub> and WP<sub>2</sub> with some common features have been reported by transport measurements.<sup>[31,32]</sup> Nevertheless, the ARPES experimental results in this family are still of absence and a large number of transports have been mainly focused on the large MR and topological surface state. Thus the anisotropic magnetic transport behaviors related with the Fermi surface structure are highly desirable to be investigated.

In this Letter, we investigate the anisotropic magnetic transports in TaSb<sub>2</sub> by measuring its MR at two different crystal directions. The large MR, metal-insulator-transition and robust resistivity plateau are observed when the magnetic field is parallel to *c*-axis and *a*-axis. The MR can follow well Kohler's rule for  $\mathbf{B} \parallel c$ , but it shows weak violation as  $\mathbf{B} \parallel a$ . The angle-dependent MR (AMR) measurements exhibit the two-fold rotational symmetry below 70 K, consistent with the monoclinic crystal structure of TaSb<sub>2</sub>. The dumbbell-like picture of AMR in TaSb<sub>2</sub> suggests a strongly anisotropic Fermi surface at low temperatures. Though this shape does not change too much below 70 K, the two-fold symmetry finally distorted as *T* is over 70 K, implying a possible topological phase transition at the characteristic temperature  $T_m$  occurring a metal-insulator-like transition under magnetic

\*Supported by the National Natural Science Foundation of China under Grant Nos 61401136, 11604299 and 61376094, the Zhejiang Natural Science Foundation of China under Grant No LY18F010019, the Open Program from Wuhan National High Magnetic Field Center under Grant No 2016KF03, and the General Program of Natural Science Foundation of Jiangsu Province under Grant No BK20171440.

\*\*Corresponding author. Email: yklee@hznu.edu.cn

© 2017 Chinese Physical Society and IOP Publishing Ltd

fields.

Single crystals of monoclinic TaSb<sub>2</sub> were grown through chemical vapor transport reaction using iodine as transport agent. The detailed synthesis procedures can be found in our previous report.<sup>[22]</sup> X-ray diffraction patterns were obtained using a D/Max-rA diffractometer with Cu  $K_{\alpha}$  radiation and a graphite monochromator at the room temperature. The single crystal x-ray diffraction determines the crystal grown orientation. The (magneto) resistivity and Hall coefficient measurements were performed using the stan-

dard four-terminal method in which the current is parallel to the  $b$ -axis. Ohmic contacts were carefully prepared on the crystal with a Hall-bar geometry. Silver wires were attached on the surface of crystals with silver paste. The low contact resistance was obtained after annealing at 573 K for an hour. The physical property was performed in a commercial Quantum Design PPMS-9 system with a torque insert with a temperature range from 2 to 300 K and the magnetic fields up to 9 T.

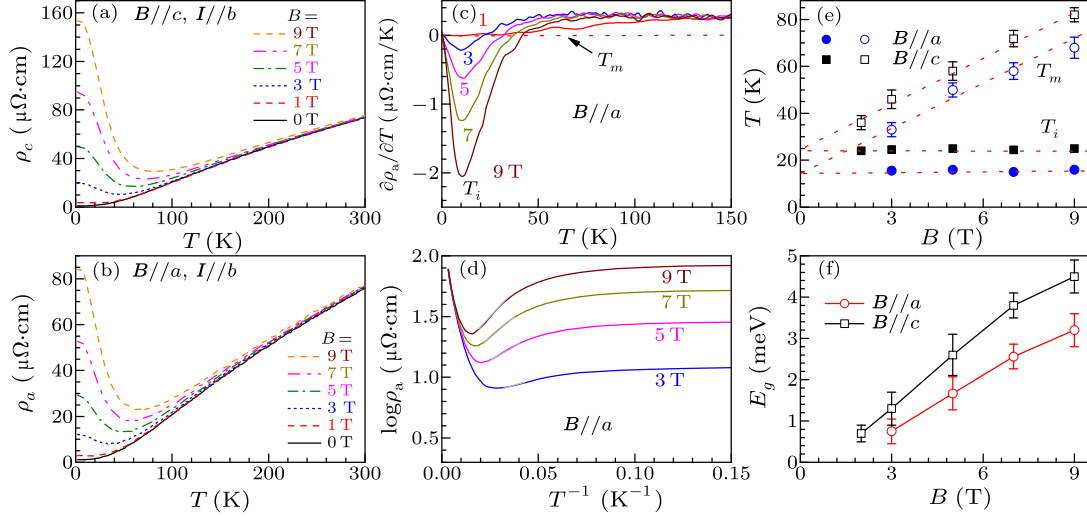


**Fig. 1.** Temperature dependence of resistivity for TaSb<sub>2</sub>. Here (a) and (b) show resistivity as a function of temperature in several magnetic fields when  $\mathbf{B}||c \perp I$  and  $\mathbf{B}||a \perp I$ , respectively. (c) Temperature dependence of  $\partial\rho/\partial T$  for  $\mathbf{B}||a$ . (d) The value of  $\log(\rho)$  plotted as a function of  $T^{-1}$ . The cyan lines show the region of the linear fits. (e) The values of  $T_m$  and  $T_i$  versus magnetic fields for  $\mathbf{B}||a$  and  $\mathbf{B}||c$ . (f) Field dependence of  $E_g$  for  $\mathbf{B}||a$  and  $\mathbf{B}||c$ . The data of  $\mathbf{B}||c$  can be found in Ref. [23].

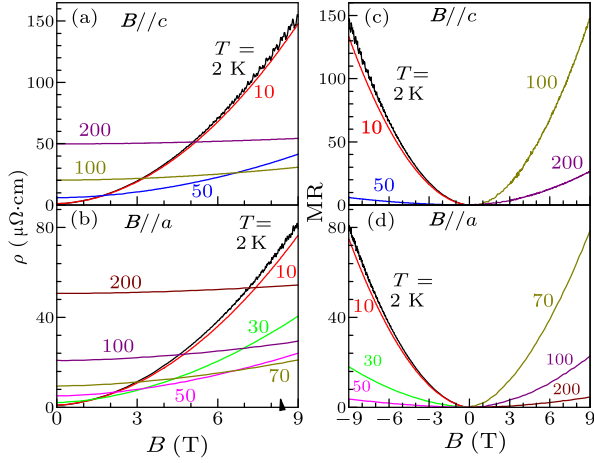
Figure 1 summarizes the magneto-transport properties of TaSb<sub>2</sub> with magnetic field along the  $c$ -axis and the  $a$ -axis. As shown in Figs. 1(a) and 1(b),  $\rho(T)$  at zero magnetic field exhibits highly metallic behavior down to 2 K, but sharply increases at low temperatures, followed by a metal-to-insulator-like transition below 70 K when the magnetic field is applied over 3 T. Such behavior has been found in the other known semimetal materials.<sup>[7,9]</sup> Further cooling temperature,  $\rho(T)$  starts to saturate at lower temperature regime, developing a resistivity plateau which has been investigated in our previous work.<sup>[22]</sup> Notice that increases in  $\rho(T)$  for  $\mathbf{B}||c$ , approaching by two times the values for  $\mathbf{B}||a$  at 9 T and 2 K, are observed, suggesting an anisotropic MR in TaSb<sub>2</sub>.

Figure 1(c) shows the temperature dependence of the derivative  $\partial\rho(T)/\partial T$  at different fields for  $\mathbf{B}||a$ . If we define  $T_m$  as the metallic to insulating behavior transition at the one with minimum  $\rho(T)$  and  $T_i$  as the onset of the plateau, it can be found that the sign change of  $\partial\rho(T)/\partial T$  and the drop peak take place at the characteristic temperatures  $T_m$  and  $T_i$ , respectively, where  $\partial\rho(T)/\partial T = 0$  and  $\partial^2\rho(T)/\partial T^2 = 0$ . As a comparison, the evolution of  $T_m$  and  $T_i$  versus  $B$  for  $\mathbf{B}||c$  as well as  $\mathbf{B}||a$  is plotted in Fig. 1(e), where  $T_m$  increases linearly but  $T_i$  remains almost

constant with the fields. Such feature implies that the insulating-like behavior is sensitive to the magnetic field while the plateau is robust and intrinsic even at zero field, similar to the case of LaSb.<sup>[33]</sup> The energy gap of insulator state  $E_g$  for  $\mathbf{B}||a$  can be obtained by fitting  $\rho(T) = \rho_0 \exp(E_g/K_B T)$ . The result of  $\log(\rho)$  as a function of  $T^{-1}$  in the range of  $T_i < T < T_m$  is plotted in Fig. 1(d). The estimated  $E_g$  values for  $\mathbf{B}||c$  are much larger than that of  $\mathbf{B}||a$ , as displayed in Fig. 1(f). This large difference further supports the large anisotropic Fermi surface in the sample. The applied magnetic fields can substantially enhance the effective mass of electrons or holes in the Dirac semimetals because of the Zeeman effect. Considering the components of the mobility tensor at the different crystal directions, the increasing resistivity with magnetic fields is expected to be the large difference for  $\mathbf{B}||a$  and  $\mathbf{B}||c$ , resulting in the greatly different energy gaps  $E_g$ .

Figure 2 plots the field dependence of the MR below 100 K for  $\mathbf{B}||c$  and  $\mathbf{B}||a$  directions, respectively. At 2 K, the resistivity increases sharply with clear Shubnikov-de Haas (SdH) oscillations as the increasing magnetic field is over 6 T in both crystal directions. Warming up temperature results in a decreasing increase in  $\rho$  under the magnetic fields. As  $T \geq 100$  K,

this curve of  $\rho$  versus  $B$  becomes flatter, indicative of a small MR at high temperatures. The large positive MR plotted in Figs. 2(c) and 2(d) is observed, reaching about 15000% and 8000% at 2 K and 9 T for  $B\parallel c$  and  $B\parallel a$ , respectively. On heating, the MR decreases monotonously with increasing temperature to 200 K where its MR is several orders of magnitude smaller than the value at 2 K. This very small MR of less than 1% at 200 K and 9 T is in contrast to most of the semimetals with a relatively large MR even at room temperature.<sup>[7,16,18,34]</sup> This behavior suggests that TaSb<sub>2</sub> is the high-metallicity at high temperatures more than others. On the other hand, the MR exhibits the quasi-quadratic for low fields and linear for larger  $B$  without saturation, analogous to many known semimetallic materials such as TaAs(P) and WTe<sub>2</sub>.<sup>[7,9–12]</sup>



**Fig. 2.** Magnetic field dependence of (magneto) resistivity in TaSb<sub>2</sub>. Here (a) and (b) show  $\rho$  versus  $B$  at different temperatures as  $B\parallel c$  and  $B\parallel a$ , respectively; (c) and (d) display the MR as a function of  $B$  for  $B\parallel c$  and  $B\parallel a$ , respectively.

The origin of large MR in some semimetals has been mainly attributed to the electron and hole compensation mechanism.<sup>[7,35]</sup> In the context, a simplified Kohler's rule:  $\text{MR} \propto (B/\rho(T, 0))^m$ , can be adopted to test the MR at distinct temperatures. On the assumption of  $T$ -independent carrier density  $n$  and the constant effect mass  $m^*$ , the MR at various temperatures can be scaled onto a single line with a constant  $m = 1$  and 2 according to this rule. Interestingly, despite the semiclassical origin of this rule, a large number of materials from conventional metals to some quantum matters including a part of topological semimetals can always follow this formula. Here we examine this rule in TaSb<sub>2</sub> as shown in Figs. 3(a) and 3(b), and find that it is well obeyed over a wide temperature range for  $B\parallel c$  but this rule is slightly violated as  $B\parallel a$ . The obtained  $m (=1.95)$  for  $B\parallel c$  is very closed to the classical value 2, while it displays a moderate  $T$ -dependent in particular violating the field-square dependence of the MR for  $B\parallel a$ , as summarized in the inset of Fig. 3(b). This divergency may be ascribed to the anisotropic Fermi surface topological structure which needs to be further investigated by ARPES measurements.

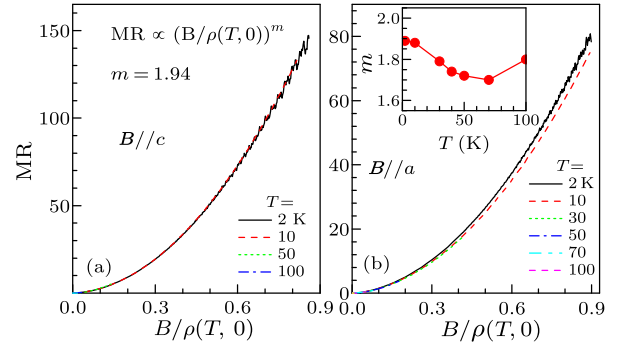


**Fig. 3.** Kohler's rule in TaSb<sub>2</sub>. MR versus  $B/\rho_0$  at several temperatures for  $B\parallel c$  (a) and for  $B\parallel a$  (b). The inset shows the fitting  $m$  values at several temperatures.

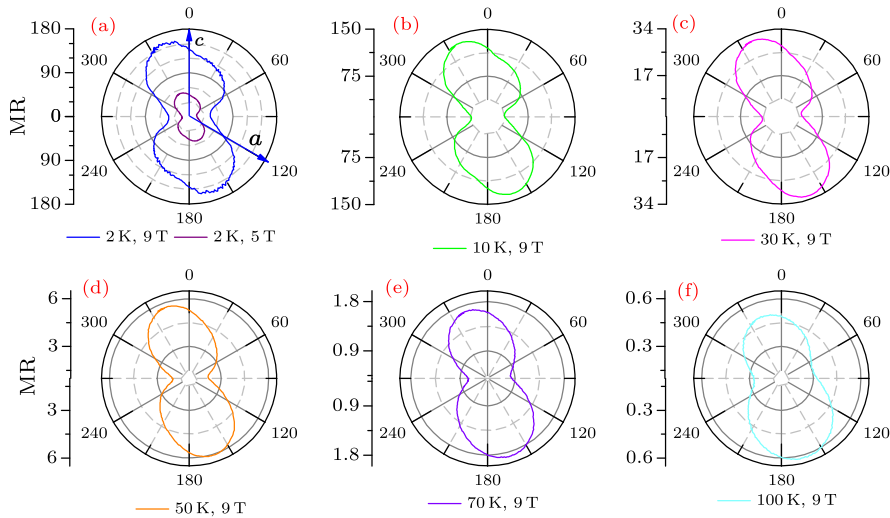


**Fig. 4.** Angle dependence of MR in TaSb<sub>2</sub>. (a) AMR at 2 K under two different magnetic fields 5 T and 9 T. (b)–(f) The AMR at different temperatures under 9 T.

Figure 4 shows the transverse MR for the TaSb<sub>2</sub> at several distinct temperatures with the rotation of field about *b*-axis. In Fig. 4(a), the picture of the AMR at 2 K shows a dumbbell-like shape under 5 T and 9 T when the field takes a turn from *c*-axis towards *a*-axis, suggesting a strongly anisotropic Fermi surface at low temperatures. Its value first decreases gradually and reaches the minimum ( $\sim 4500\%$ ) at around  $\theta \sim 80^\circ$ . With further increasing the angle, the MR starts to increase reversely, displaying a maximum value of 16500% at 9 T at around  $165^\circ$ . The pattern of AMR shows a two-fold rotational symmetry. Both the maximum and the minimum values of MR repeat again for one turn. As  $\mathbf{B} \parallel a$  and  $\mathbf{B} \parallel c$ , the corresponding values in the AMR appear exactly four times and two times, respectively. Those results are highly in agreement with the monoclinic crystal structure of TaSb<sub>2</sub>. Notice that the position of the maximum and the minimum value does not match the *c*-axis and *a*-axis directions of single crystallography, implying a complex Fermi surface topological structure. On heating temperature under a constant field of 9 T, the AMR decreases monotonously, meanwhile the pattern of the dumbbell-like shows the slight change below 50 K, but starts to lose the two-fold rotational symmetry above 70 K, where the characteristic temperature  $T_m$  (reported in the previous work<sup>[22]</sup>) reminds us of the metal to insulator-like transition in resistivity at 9 T. The evolution of the AMR with temperature may be ascribed to a possible topological phase transition, like MoTe<sub>2</sub>,<sup>[35]</sup> WTe<sub>2</sub><sup>[36,37]</sup> and MoAs<sub>2</sub>.<sup>[31]</sup>

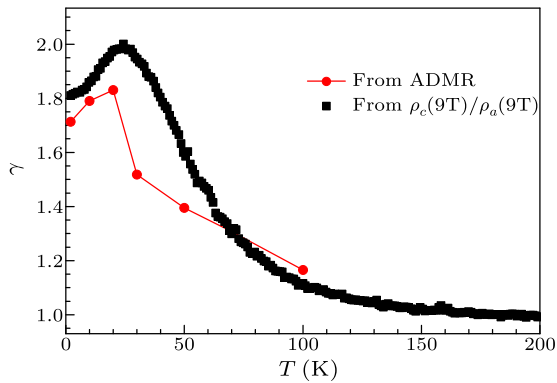


Fig. 5. Temperature dependence of anisotropic value  $\gamma$ .

According to the above investigated experimental results, we can summarize the evolution of temperature dependence of anisotropy value  $\gamma$  ( $= \rho_c(9T)/\rho_a(9T)$ ) in Fig. 5. We find that at low temperatures the sample exhibits an obviously anisotropic MR ( $\sim 2$ ). With increasing temperature, the anisotropic value shows a peak at around 20 K, and then decreases sharply to  $\sim 1$  above 70 K. This temperature-dependent  $\gamma$  suggests that the increase of MR in  $\mathbf{B} \parallel c$  is larger than that of in  $\mathbf{B} \parallel a$  below 70 K, implying the anisotropic Fermi surface structure in TaSb<sub>2</sub>. Moreover, the quick increase of  $\gamma$  together with the lost two-fold symmetry below 70 K points to

a possible change of Fermi surface topological structure occurring around the temperature.

In summary, we have investigated the anisotropic MR of TaSb<sub>2</sub> below 100 K by measuring the MR for  $\mathbf{B} \parallel c$  and  $\mathbf{B} \parallel a$  directions, and the AMR below 100 K at 9 T. It is found that the sample shows the unsaturated large MR with linear-dependence at high magnetic fields, the increasing metal-insulator-like transition ( $T_m$ ) below 70 K and robust resistivity plateau ( $T_i$ ) with magnetic fields when  $\mathbf{B} \parallel c$  and  $\mathbf{B} \parallel a$ . The MR follows Kohler's rule very well for  $\mathbf{B} \parallel c$  but slightly violates this rule as  $\mathbf{B} \parallel a$  direction, implying a complex Fermi surface in the present sample. The AMR displays two-fold rotational symmetry below 70 K, consistent with the monoclinic crystal structure of TaSb<sub>2</sub>. A dumbbell-like picture of AMR in TaSb<sub>2</sub> suggests a strongly anisotropic Fermi surface at low temperatures. It gradually changes the shape very weakly but finally loses the two-fold symmetry above 70 K, implying a possible topological phase transition at around the characteristic temperature where  $T_m$  undergoes a metal-insulator-like transition under magnetic field.

## References

- [1] Pippard A B 1989 *Magnetoresistance in Metals* (Cambridge: Cambridge University)
- [2] Moritomo Y, Asamitsu A, Kuwahara H and Tokura T 1996 *Nature* **380** 141
- [3] Doughton J M 1999 *J. Magn. Magn. Mater.* **192** 334
- [4] Baibichet M, Broto J M, Fert A, VanDau F N, Petro F, Etienne P, Creuzet G, Friederich A and Chazelas J 1988 *Phys. Rev. Lett.* **61** 2472
- [5] Salamon M B and Jaime M 2001 *Rev. Mod. Phys.* **73** 583
- [6] Jeon S, Zhou B B, Gyenis A, Feldman B E, Kimchi I, Potter A C, Gibson Q D, Cava R J, Vishwanath A and Yazdani A 2014 *Nat. Mater.* **13** 851
- [7] Ali M N, Xiong J, Flynn S, Tao J, Gibson Q D, Schoop L M, Liang T, Haldolaarachchige N, Hirschberger M, Ong N P and Cava R J 2014 *Nature* **514** 205
- [8] Weng H, Fang C, Fang Z, Bernevig B A and Dai X 2015 *Phys. Rev. X* **5** 011029
- [9] Huang S M, Xu S Y, Belopolski I, Lee C C, Chang G, Wang B, Alidoust N, Bian G, Neupane M, Zhang C, Jia S, Bansil A, Lin H and Hasan M Z 2015 *Nat. Commun.* **6** 7373
- [10] Zhang C, Yuan Z, Xu S, Lin Z, Tong B, Hasan M Z, Wang J, Zhang C and Jia S 2017 *Phys. Rev. B* **95** 085202
- [11] Xu S Y, Belopolski I, Alidoust N, Neupane M, Bian G, Zhang C, Sankar R, Chang G, Yuan Z, Lee C C, Huang S M, Zheng H, Ma J, Sanchez D S, Wang B, Bansil A, Chou F, Shibaev P P, Lin H, Jia S and Hasan M Z 2015 *Science* **349** 613
- [12] Lv B Q, Weng H M, Fu B B, Wang X P, Miao H, Ma J, Richard P, Huang X C, Zhao L X, Chen G F, Fang Z, Dai X, Qian T and Ding H 2015 *Phys. Rev. X* **5** 031013
- [13] Ghimire N J, Luo Y, Neupane M, Williams D J, Bauer E D and Ronning F 2015 *J. Phys.: Condens. Matter* **27** 152201
- [14] Xu S Y, Alidoust N, Belopolski I, Yuan Z, Bian G, Chang T R, Zheng H, Strocov V N, Sanchez D S, Chang G, Zhang C, Mou D, Wu Y, Huang L, Lee C C, Huang S M, Wang B, Bansil A, Jeng H T, Neupert T, Kaminski A, Lin H, Jia S and Hasan M Z 2015 *Nat. Phys.* **11** 748
- [15] Shekhar C, Nayak A K, Sun Y, Schmidt M, Nicklas M, Leermakers I, Zeitler U, Skourski Y, Wosnitza J, Liu Z, Chen Y, Schnelle W, Borrmann H, Grin Y, Felser C and Yan B 2015 *Nat. Phys.* **11** 645
- [16] Arnold F, Shekhar C, Wu S C, Sun Y, Reis R D, Kumar N, Naumann M, Ajeesh M O, Schmidt M, Grushin A G, Bar-

- darson J H, Baenitz M, Sokolov D, Borrmann H, Nicklas M, Felser C, Hassinger E and Yan B **2016** *Nat. Commun.* **7** 11615
- [17] Zhang J, Liu F L, Dong J K, Xu Y, Li N N, Yang W G and Li S Y **2015** *Chin. Phys. Lett.* **32** 097102
- [18] Schoop L M, Ali M N, Strar C, Duppel V, Parkin S S P, Lotsch B V and Ast C R **2016** *Nat. Commun.* **7** 11696
- [19] Hu J, Tang Z, Liu J, Liu X, Zhu Y, Graf D, Myhro K, Tran S, Lau C N, Wei J and Mao Z **2016** *Phys. Rev. Lett.* **117** 016602
- [20] Abrikosov A A **1998** *Phys. Rev. B* **58** 2788
- [21] Liang T, Gibson Q, Ali M N, Liu M, Cava R J and Ong N P **2014** *Nat. Mater.* **14** 280
- [22] Li Y K, Li L, Wang J L, Wang T, Xu X, Xi C, Cao C and Dai J **2016** *Phys. Rev. B* **94** 121115
- [23] Wang Y Y, Yu Q H, Guo P J, Liu K and Xia T L **2016** *Phys. Rev. B* **94** 041103
- [24] Wu D S, Liao J, Yi W, Wang X, Li P, Weng H, Shi Y G, Li Y, Luo J, Dai X and Fang Z **2016** *Appl. Phys. Lett.* **108** 042105
- [25] Luo Y K, McDonald R D, Rosa P F S, Scott B, Wakeham N, Ghimire N J, Bauer E D, Thompson J D and Ronning F **2016** *Sci. Rep.* **6** 27294
- [26] Yuan Z J, Lu H, Liu Y, Wang J and Jia S **2016** *Phys. Rev. B* **93** 184405
- [27] Shen B, Deng X Y, Kotliar G and Ni N **2016** *Phys. Rev. B* **93** 195119
- [28] Li Y P, Wang Z, Lu Y, Yang X, Shen Z, Sheng F, Feng C M, Zheng Y and Xu Z A **2016** [arXiv:1603.04056](#) [cond-mat.str-el]
- [29] Wang K F, Graf D, Li L J, Wang L M and Petrovic C **2015** *Sci. Rep.* **4** 7328
- [30] Xu C, Chen J, Zhi G X, Li Y, Dai J and Cao C **2016** *Phys. Rev. B* **93** 195106
- [31] Wang J L, Li L, You W, Wang T T, Cao C, Dai J H and Li Y K **2016** [arXiv:1610.08594](#) [cond-mat.mtrl-sci]
- [32] Kumar N, Sun Y, Xu N, Manna K, Yao M, Suess V, Leermakers I, Young O, Foerster T, Schmidt M, Yan B H, Zeitler U, Shi M, Felser C and Shekhar C **2017** [arXiv:1703.04527](#) [cond-mat.mtrl-sci]
- [33] Tafti F F, Gibson Q D, Kushwaha S K, Haldolaarachchige N and Cava R J **2015** *Nat. Phys.* **12** 272
- [34] Wang Y Y, Yu Q H and Xia T L **2016** *Chin. Phys. B* **25** 107503
- [35] Zhou Q, Rhodes D, Zhang Q R, Tang S, Schnemann R and Balicas L **2016** *Phys. Rev. B* **94** 121101
- [36] Wu Y, Jo N H, Ochi M, Huang L, Mou D X, Bud'ko S L, Canfield P C, Trivedi N, Arita R and Kaminski A **2015** *Phys. Rev. Lett.* **115** 166602
- [37] Pletikosi I, Ali M N, Fedorov A V, Cava R J and Valla T **2014** *Phys. Rev. Lett.* **113** 216601